

## UNSATURATED FLOW IN POROUS MEDIA

C.L. Bronisz and C.W. Hirt  
Flow Science Inc.

January 1991/Revised July 1996/July 2005

### OVERVIEW

Unsaturated flow in porous media involves many complex phenomena not present under saturated flow conditions. For instance, there are free boundaries whose configurations are unknown, and capillary forces exist that may generate large negative pressures pulling fluid into less saturated regions. Additionally, the capillary pressures may exhibit hysteresis behavior that makes their experimental determination and modeling more difficult.

The complications associated with unsaturated flows dictate the need for numerical solution procedures in all but the simplest of situations. Because of the free surface aspects of these types of flows, it is natural to think of extending the *FLOW-3D*<sup>®</sup> program to the general case of unsaturated flow. The modifications necessary to do this extension are described in this report.

As explained more fully in later sections, it is necessary to have sufficient empirical data about a porous substance and the liquid penetrating it in order to correctly model flow through the substance. The models reported here for capillary pressures and permeability have a generic character that may require modification for some materials.

### THE *FLOW-3D*<sup>®</sup> PROGRAM

*FLOW-3D*<sup>®</sup> is a finite-difference formulated solution algorithm for the fluid conservation equations of mass, momentum, and energy. It is fully three dimensional and time dependent. The code uses a rectangular (or cylindrical) grid of control volumes for discretizing the conservation equations. In order to model situations having complicated geometry consisting of curved or slanted surfaces, the code uses a porosity technique called FAVOR<sup>™</sup> (Fractional Area/Volume Obstacle Representation method). The general idea of FAVOR<sup>™</sup> is to define the fractional face areas and fractional volume of each computational control volume that is open to flow. Equations containing this information are analogous to the equations for flow in porous media.

Because of the FAVOR<sup>™</sup> formulation, *FLOW-3D*<sup>®</sup> possesses the necessary porosity variable (VF) for representing a continuous porous medium. Of course, we then must be careful not to confuse the representation of obstacles with that of porous media. Since the basic characteristics of a porous flow region is a Darcy-like flow resistance (or permeability), it is possible to use the FAVOR<sup>™</sup> scheme for both situations simultaneously provided the permeability is correctly defined.

*FLOW-3D*<sup>®</sup> also has a powerful capability for the tracking of free fluid boundaries. For this purpose it uses a variable, F, representing the fraction of open volume that is occupied by liquid. In porous media terminology, F is the saturation.

A momentum drag term proportional to the velocity (Darcy term) is contained in **FLOW-3D**<sup>®</sup>. This term represents the average shear stresses experienced by fluid as it passes through the small open pores of the medium. In typical applications this drag is so large that inertial effects are negligible, and the momentum equations reduce to Darcy's formulation, i.e., a balance between drag and pressure gradients (including gravitational body forces).

In practice, the reciprocal of the drag is used in the code, since this quantity maintains a value between one and zero while the drag itself varies between zero and infinity, respectively. As presently formulated in **FLOW-3D**<sup>®</sup> the permeability-like variable, DRG, has no dimensions. On the other hand, the drag coefficient, K, has dimensions of inverse time. The formal relation between these quantities is contained in the code subroutine *DRGCLF* and is expressed as,

$$DRG = \frac{1}{1 + \delta t K}$$

where the first term in the denominator is associated with fluid inertia and is usually negligible with respect to the second term in a porous media. The factor  $\delta t$  is the time-step integration size used for advancing the solution in time. In the limit of Darcy flow (i.e.,  $\delta t K \gg 1$ ) the fluid velocity is given by

$$\vec{u} = \frac{1}{K} \left( -\frac{1}{\rho} \nabla p + \vec{g} \right)$$

where  $\vec{g}$  is the acceleration of gravity,  $p$  is fluid pressure and  $\rho$  is the fluid density.

We can relate the drag coefficient K to a permeability or hydraulic conductivity as used in the literature in the following way:

$$\text{Hydraulic Conductivity} = Fng/K \quad [\text{Units L/T}]$$

$$\text{Permeability} = Fnv/K \quad [\text{Units L}^2]$$

Where F is the saturation or fraction of available volume occupied by fluid, n is the porosity ( $n=VF$ ), g the acceleration of gravity magnitude and v the fluid kinematic viscosity.

With the original formulation of **FLOW-3D**<sup>®</sup> it is possible to model flow in porous media under conditions where there are no capillary effects, for example, when a liquid front moves into a dry zone so rapidly that a capillary-driven precursor does not have time to develop. This may occur, for example, when the capillary pressure is small compared to pressures in the fluid or when flow resistance in the media is small enough that liquid can rapidly fill all newly wetted regions. The free surface of the liquid in this case is a sharp transition between fully saturated and zero saturated conditions.

To extend the **FLOW-3D**<sup>®</sup> models to include unsaturated flow effects several modifications must be made. These are described in the next section.

## MODEL EXTENSIONS

Capillary effects imply the possibility of diffuse boundaries between dry and fully saturated conditions. In regions where unsaturated conditions exist the effective fluid pressure is strongly affected by capillary forces and there may be a nonzero velocity divergence (i.e., a net flow of liquid in or out of the region). Furthermore, the capillary pressure may depend on the previous history of filling or draining the region.

Complicating the modeling of unsaturated flows is the fact that the functional dependencies of capillary pressure and permeability on saturation are often highly nonlinear.

### Model Activation

The unsaturated flow model in **FLOW-3D**<sup>®</sup> is activated by the parameter *IDRG=5*. *IDRG* is the flag for the incorporation of a momentum drag term and the value assigned to *IDRG* is used to determine the type of drag expression to use. The value *IDRG=5* tells the code to evaluate a drag only in those mesh zones where the volume fraction (porosity) is less than a value slightly less than 1.0 (e.g., 1.0 -1.0e-6). This choice allows for a region of free liquid flow (volumes fraction 1.0) adjacent to the porous media.

### Drag or Permeability

The drag, *K*, is defined to be the product of a saturated drag coefficient, *K<sub>0</sub>*, and an unsaturated correction factor. The saturated drag, *K<sub>0</sub>*, has been defined as *OADRG*, an input parameter for each porous obstacle. The reciprocal of this expression (i.e., permeability) is referred to as the Kozeny-Carman relation (Ref. 1, p.166)

$$K_0 = OADRG = 180\nu \left(\frac{1-n}{n}\right)^2 \frac{1}{d^2}$$

where  $\nu$  is the liquid kinematic viscosity,  $n$  is the porosity and  $d$  is some average diameter of the particles. *OADRG* is selected to match experimental data. Note: Sometimes there is an  $n^3$  in the denominator instead of the  $n^2$  as written above. This difference is necessary when the drag is defined by the product of *K<sub>0</sub>* times the macroscopic flow velocity  $\mathbf{u}$ . In the current formulation the drag is *K<sub>0</sub>* times the microscopic velocity  $\mathbf{u}$ , which necessitates the  $n^2$  version.

With the addition of the correction factor for unsaturated flow, the drag coefficient is given by either of two forms, which are selected by the input variable *IDFIT*.

$$K = \frac{K_0}{S_e^B}, \quad IDFIT = 1$$

or

$$K = K_0 \frac{e^{B(1-S_e)}}{S_e^{p_{exp}}} \left( \frac{F}{F - F_{cmm}} \right), \quad IDFIT = 2$$

where *B* is an exponent that must be determined empirically. Parameter *B* is specified as input quantity *OBDRG* for each porous obstacle.  $S_e$  the effective saturation defined as,

$$S_e = \frac{(F - F_{cmn})}{(1 - F_{cmn})}$$

where  $F_{cmn}$  is an experimentally determined “irreducible” saturation ( $F_{cmn}=0.0$  is the default). The exponent  $p_{exp}$  is another experimentally determined constant that is also used to relate saturation to capillary pressure (see discussion of capillary pressure below). The above expressions for drag as a function of  $S_e$  have been verified for many types of porous media. For example, in a close-packed bed of equal pore sizes it can be shown that  $B=3$  for  $IDFIT=1$ .

There is some evidence that drag (permeability) is subject to hysteresis effects similar to those observed in the capillary pressure. Because little is known about this, we have chosen to simply approximate this complication in the present model.

Experience dictates that the drag must be large (or permeability low) when the level of saturation is low. This implies that the exponent,  $B$ , must be positive. In general, it is further observed (Ref. 1, p.4910 that in granular solids the permeability should have a zero (or small positive) slope with respect to saturation at the limit of irreducible saturation. This then implies that  $B$  must be greater than or equal to 1.0.

### Capillary Pressure

The capillary pressure is also a function of effective saturation. For most cases it is necessary to determine this function by experimental means. Unfortunately, the functional dependence exhibits a hysteresis when the porous medium is cycled between filling and draining (see Fig. 1).

For a given process, say draining, it has been observed that the capillary pressure  $P_c$ , can be closely approximated by a power of the effective saturation for many different types of porous media (Ref. 1 pp. 446 and 465),

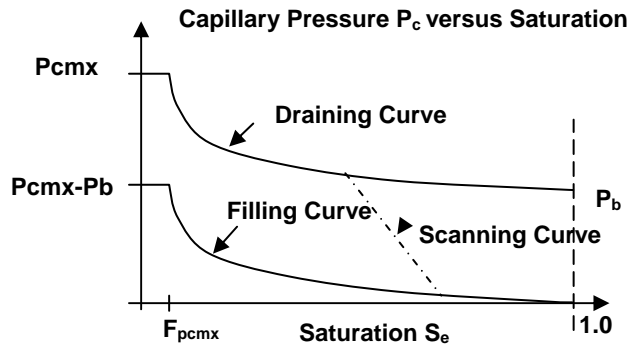


Figure 1. Capillary Pressure vs. Saturation

$$P_c = \frac{P_b}{S_e^{p_{exp}}}$$

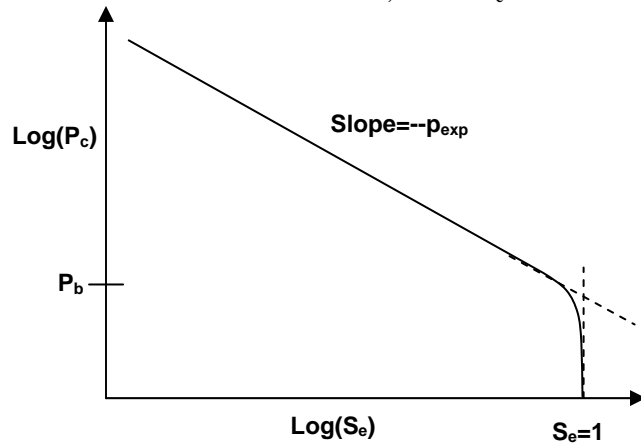
where  $P_b$ , a constant, is called the “bubbling” pressure (see Fig.2). Actually, this power-law expression is not accurate at very low or very high values of saturation, as explained in more detail below.

When hysteresis effects are present, there will be two such relations for  $P_c$ . One corresponds to filling and the other to draining of the porous media.

A further complication may exist if the medium is not uniform, for then the pressure versus saturation relation may depend on location. This complication has been partially addressed by

allowing users to input multiple geometry regions, each region having its own porous media properties.

It is clear that the above expressions for drag and capillary pressure cannot be correct for all values of saturation. For instance,  $K$  and  $P_c$  become infinite as  $S_e$  approaches zero, which is not



physically meaningful. Also, for filling we would expect  $P_c$  to be zero at  $S_e=1$ , and not  $P_b$  since there are no free surfaces in this limit.

One further problem is associated with the effective saturation. The concept of an irreducible saturation  $F_{cmn}$ , is associated with the idea that a porous medium cannot be completely drained by pressure forces. That is, some

Figure 2. Capillary Pressure vs saturation

fraction of liquid will remain trapped in internal pockets or crevices as isolated blobs of liquid. On the other hand, when filling a porous material, it is not uncommon for the material to be initially dry (i.e.,  $F=0$ ). In this case some adjustment must be made in the definition of  $S_e$  until  $F$  exceeds  $F_{cmn}$ .

In *FLOW-3D*<sup>®</sup> we have handled these limiting cases in several ways described in the following sections.

### Low Saturation Limit

At low saturation the capillary pressure can be quite large. Since we must rely on experimental data for capillary pressure versus saturation relation, we shall set the maximum value of  $P_c$  equal to the maximum value,  $P_{cmx}$ , that is measured at the lowest saturation  $F=F_{pcmx}$ .

When evaluating  $P_c$  for the draining curve, the  $F$  appearing in the power-law expression is never allowed to be less than  $F_{pcmx}$ . Thus we have  $P_c=P_{cmx}$  for all  $F$  values less than or equal to  $F_{pcmx}$ . A similar situation is also true for the filling curve.

Note that the irreducible saturation,  $F_{cmn}$ , must always be less than  $F_{pcmx}$ . If  $F_{cmn}$  is not specified, it defaults to zero. Also, whenever  $S_e$  is evaluated, the  $F$  value used in the evaluation is never less than  $F_{pcmx}$  (i.e.,  $S_e$  is never allowed to reach zero).

### Full Saturation Limit

At the limit of full saturation,  $S_e=1$ , the drag coefficient attains its fully saturated value,  $K_0$ , which is another empirical constant (actually a function of porosity).

On the other hand, the model for capillary pressure limits to  $P_b$  at full saturation. This limit is correct for draining, but not for filling. The bubbling pressure concept is a result of the power-law assumption and has been given the interpretation of the pressure needed before air can penetrate into the surface of a fully saturated porous medium. The reasoning behind this is that some

threshold pressure must be reached to sufficiently deform the surface menisci before air penetration into the pores of the medium can occur. Actual experimental data (e.g., Ref 1, p.449) indicates that the capillary pressure in reality drops rapidly to zero as full saturation is attained.

### Draining Curve versus Filling Curve

Because we feel that  $P_c$  should be zero at full saturation for filling, we have elected to modify the capillary pressures for the filling curve, as shown in Figure 1. The filling curve follows the power-law relationship defined for the draining curve, but is offset by the value of  $P_b$ , so that  $P_c$  is zero at full saturation. This means that the user specifies the draining curve, and then **FLOW-3D**<sup>®</sup> calculates the filling curve. Another input variable (*IPCFD*) can tell the code to use separate filling and draining curves (i.e., hysteresis, *IPCFD*=0), or ignore hysteresis and use either the filling curve (*IPCFD*=1) for both filling and draining or the draining curve (*IPCFD*=2) for both filling and draining.

### Motion of a Wetting Front

When fluid moves into a region of low saturation, it may do so with an almost discontinuous jump in saturation. The motion of such a jump, or wetting front as it is sometimes called, can be difficult to represent by discrete numerical approximations.

A qualitative understanding of how a jump may form may be found in the equation for the velocity of the front. Using the power-law relations for capillary pressure and drag as functions of effective saturation, and assuming the saturation is much smaller ahead of the front than behind it, the velocity is approximately given by,

$$u = \left( \frac{2P_b}{\rho K_0 \delta x} \right) S_e^{B - P_{exp}}$$

where  $\delta x$  is a mesh size. In this expression  $S_e$  is the smallest value of  $S_e$  on either side of the front, but it can be no smaller than the cutoff limit obtained when  $F=F_{cmin}$ .

When the exponent of  $S_e$  is greater than unity, the velocity at the front will be smaller than the velocity immediately behind the front where the saturation is higher. This leads to a steepening of the front much like the development of a shock wave in compressible fluids.

Conversely, when  $B$  is less than  $P_{exp}$ , the velocity will increase as  $S_e$  decreases. Thus, the velocity at the front will be larger than behind it, which results in a rapidly diffusing front having no discontinuities.

This qualitative discussion shows that the character of flow into a relatively dry region can vary significantly with the functional dependence of drag and capillary pressure on saturation. In this respect, simple experiments can provide useful information regarding this dependence.

Another important conclusion can be drawn from the above approximation expression for the wetting front velocity. If exponent  $B$  is too large with respect to exponent  $P_{exp}$ , the velocity will be nearly zero at the front. In fact, in the limit of vanishing  $S_e$  this model indicates that the front is unable to move into dry material.

To alleviate this difficulty, we have modified the drag coefficient calculation. In all unsaturated cells the  $F$  value used to evaluate the drag is weighted with the maximum  $F$  value existing in the

six neighboring cells. When the face area between a cell and its neighbor is zero this neighbor cell is not included in the search for a maximum value. Finally, the value of  $F$  used to compute the drag is  $(F+F_{\max})/2$ .

In this way the drag coefficient evaluated across a jump-type wetting front is more continuous and computations proceed without difficulty. The price paid for this improvement is some spatial smoothing of jumps in saturation, however the smoothing is not excessive and is unlikely to cause problems.

### Transition between Draining and Filling Curves

If a simulation is expected to involve only the filling or draining of a region, then it is only necessary to consider the appropriate capillary pressure-versus-saturation curve. However, when there are alternating filling and draining transients, then both curves must be considered and some means must be provided in the model for a transition between these processes. Experimentally it is observed that the transition occurs along a “scanning” curve, Figure 1. This curve must have a slope that is larger than either the filling or draining curves, otherwise it would not be possible to pass from one to the other. Because no experimental data has been found for guidance, we have arbitrarily set the slope of the scanning curve. We use a value equal to the slope of the draining curve at the current value of  $F$  plus an additional slope computed as the difference between the filling and draining curve pressures at saturation  $F$  divided by a change in saturation of 0.1.

When evaluating  $P_c$ , which is done in subroutine *PCAPCLF*, a first guess for the new capillary pressure at time step  $n+1$  is obtained from the previous time-step value by assuming a variation along a scanning curve,

$$P_c^{n+1} = P_c^n + \frac{dP_c}{dF} (F^{n+1} - F^n)$$

where  $(dP_c/dF)$  is the slope of the scanning curve. The new value is then tested against the filling and draining curve values  $(P_c^{\text{fill}}, P_c^{\text{drain}})$  such that

$$P_c^{n+1} = \max(P_c^{n+1}, P_c^{\text{fill}})$$

$$P_c^{n+1} = \min(P_c^{n+1}, P_c^{\text{drain}})$$

These tests keep the capillary pressure between the limits imposed by the two curves, or in the case of only one curve, keeps  $P_c$  on that curve.

### **ADDITION OF MODELS TO *FLOW-3D*<sup>®</sup>**

To simulate unsaturated flow conditions in *FLOW-3D*<sup>®</sup>, we assume this to be an extension of the model for a single, incompressible fluid with a free surface. From a saturation point of view, the original model corresponds to full saturation in fluid-occupied regions and zero saturation elsewhere. The free surface is a surface of discontinuity in the saturation. In this original mode the code imposes a zero velocity divergence (i.e., incompressibility condition) on all mesh cells occupied by fluid. Also, a pressure boundary condition is used at the free surface.

For unsaturated flow two important modifications must be made to the above treatment. First, we must allow for regions of fluid at less than full saturation. In these regions the pressure will be assumed given by a capillary pressure versus saturation relation. Secondly, the velocity divergence must be nonzero in unsaturated regions so that the saturation level can change as more or less fluid flows into a region. The gas pressure in any unsaturated region is always assumed to remain at a constant value of *PVOID*.

Of course, in fully saturated regions the velocity divergence must still be zero, and in these regions the pressure is determined in such a way to insure this condition. For computational purposes we shall define a saturation value of *F* within 1.0e-6 of 1.0 as the transition point between a fully saturated region and an unsaturated region.

In our first attempt to add unsaturated flow conditions to *FLOW-3D*<sup>®</sup> we simply set the pressure in every unsaturated mesh cell to be equal to its capillary pressure. This led to a workable algorithm provided the time-step size was sufficiently small. Unfortunately, the time-step size needed was typically more than an order of magnitude smaller than that needed for computational stability in the original code. The reason for a small time-step size was traced to a sensitivity of the saturation variable to gradients in saturation. For instance, if a mesh cell has a slightly larger saturation value than its neighbors, the momentum equation (Darcy's law) will generate outflow velocities at all faces of the cell. If the time step is too large, these velocities will over-empty the cell so that on the following time step it will have a saturation less than its neighbors. Then the reverse process will occur; flow velocities are directed into the cell from all neighbors and the cell overfills during the next time step. This process repeats on successive time steps to produce a very irregular distribution of saturation. Only when the time-step size is sufficiently small, can the over-filling and over-emptying processes be kept under control.

To correct for this algorithm deficiency it is necessary to use a semi-implicit method for computing capillary pressures in unsaturated regions. The basic idea is to use a pressure to compute velocities that is closer to that expected at the end of the time cycle as opposed to using the pressure at the beginning of the cycle as described above. For example, if the saturation in a cell is larger than its neighbors, it should drive a net flow out of the cell but not so much that the resulting saturation in the cell is less than its neighbors. By using the saturation expected at the end of the cycle, the resultant saturation cannot then be less than all the neighbors because that would imply inflow and not outflow velocities from the cell.

The semi-implicit method can be understood from the following argument. We need an equation that will approximate the time-advanced capillary pressure in unsaturated regions. For this we will begin with the exact relation,

$$p = P_c(F^{n+1})$$

where the right side is the capillary pressure evaluated as a function of the saturation at the new time level *n+1*. This new saturation value can be evaluated from the mass conservation equation,

$$F^{n+1} = F^n - \delta t \nabla \cdot (F^n \vec{u}^{n+1})$$

For small  $\delta t$  we can expand the right side of the pressure equation in a Taylor series,

$$p = P_c(F^n) + \frac{dP_c}{dF}(F^{n+1} - F^n) + \dots$$

where  $P_c(F^n)$  is simply the current time pressure,  $p^n$ , in unsaturated regions. Substituting for the  $F$  change from the mass equation,

$$p = p^n - \frac{dP_c}{dF} \delta t \nabla \cdot (F^n \vec{u}^{n+1})$$

where only the first order Taylor series term is retained. Now the divergence term can be expanded using the relation,

$$\nabla \cdot (F\vec{u}) = \vec{u} \cdot \nabla F + F \nabla \cdot \vec{u}$$

It is the second term on the right side of this expression that causes  $F$  to undergo large increases or decreases. If we approximate the other term using old, time  $n$  velocities, the resulting approximation for  $p$  is then,

$$p = p^n - \frac{dP_c}{dF} \delta t (F^n \nabla \cdot \vec{u}^{n+1} + \vec{u}^n \cdot \nabla F^n)$$

Rewriting this result, we finally obtain the desired result,

$$\frac{1}{F^n (dP_c / dF)} \frac{(p - p^n)}{\delta t} + \nabla \cdot \vec{u}^{n+1} = -\vec{u}^n \cdot \frac{\nabla F^n}{F^n}$$

This expression looks like a limited compressibility equation with a bulk compressibility of

$$F^n \frac{dP_c}{dF}$$

and having an explicit source term on the right hand side. In fully saturated regions we must eliminate the first term from this equation, which involves  $p$  as well as the term on the right side, so that the resulting equation becomes the incompressibility condition.

Thus, if we used the above expression in unsaturated regions, the result will be an approximation to the time  $n+1$  capillary pressure. To use this prescription in **FLOW-3D**<sup>®</sup> is quite easy because the code is already designed to handle limited compressibility. The only additions needed are to correctly define the bulk compressibility and right-hand side source term for the next cycle of computation.

Using this algorithm we find that the code works very well with a time-step size close to that needed in the original code to satisfy other types of computational stability requirements. The only recommendation is that the stability condition for advection be tightened by a factor of two, which helps to keep the filling and emptying of cells smoother. This tightening is automatically done by the code when the unsaturated models are requested.

A factor of two reduction in the advection stability is suggested because the usual default limit is on the borderline of stability. The borderline limit generally works because advection is typically a unidirectional process. On the other hand, in unsaturated flow the velocities tend to be all directed toward or away from low or high values of saturation, respectively, which emphasizes the filling and emptying processes.

## COMPUTATIONAL EXAMPLES

As a demonstration of the new unsaturated flow capability, we present results from a few simple examples. The first example is compared with experimental data, while the others illustrate some properties of unsaturated flow in porous media.

### Movement of Water in Soil

A good test of unsaturated flow is the diffusion of water into soil. Unfortunately, good physical data is hard to come by. A search uncovered data for a one-dimensional flow of water into a horizontal column of Traver sandy loam (W.R. Gardner and M.S. Mayhugh, "Solutions and Tests of the Diffusion Equation for the Movement of Water in Soil," Soil Science Soc. Amer. Proc. **22**, 197, 1958). The experimental data confirm that it is acceptable to use a power-law relation between capillary pressure and saturation as well as an exponential form of flow drag versus saturation. Using the published data one can compute the input required for *FLOW-3D*<sup>®</sup> to represent this particular soil material:

```
OADRG=1.39e+4
OBDRG=9.425,
  OPOR=0.3626
FPCMX=0.12
  PCMX=2.62E+4
  PEXP=0.5
  IDR=5
  IDFIT=2
  IPCFD=0
```

The one-dimensional flow channel had lateral dimensions 1.8cm by 1.3cm and a length of 24.25cm, which was sufficient to follow the water penetration for 4860s (81min). The soil was given an initial saturation of 0.12 volume fraction (or 7% water by weight). Fully saturated conditions were specified at the left end of the column as a boundary condition. The computational grid consisted of 97 uniform elements along the channel.

Figure 3 shows a comparison of the computed and measured water concentrations (% by weight) at the end of the simulation (t=81min). We see there is good agreement; even at the front where the saturation increase is very steep, a consequence of the highly nonlinear dependence of drag

and capillary pressure on saturation.

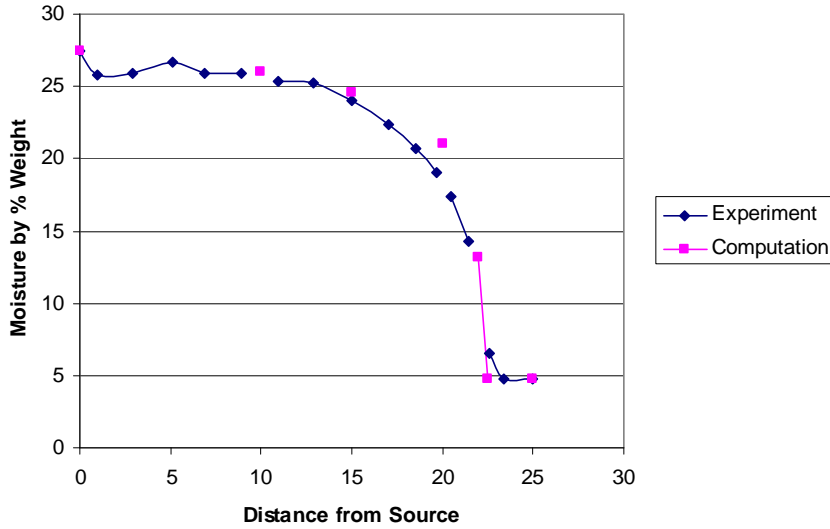


Figure 3. Flow into Traver Sandy Loam, at  $t=81$ min.

#### Uniform Wetting of Porous Media

One feature of unsaturated flow in a finite piece of porous media is that any liquid should eventually diffuse more or less to a uniform saturation. Even if some region is initially at 100% saturation, its surface should be able to diffuse into surrounding regions having a lower saturation. From the equations of motion, this behavior is not obvious because in a fully saturated region the velocity divergence should be zero to preserve incompressibility of the fluid. On the other hand, there is no incompressibility restriction that prevents a 100% saturated region from losing fluid to a neighboring region at a lower saturation. To test whether or not our model is consistent with this situation we used the previous setup but with the left boundary replaced by a wall and with a central region of the channel given an initial saturation of 100%.

A short computation shows that the edges of the fully saturated region do diffuse out into the surrounding region, Figure 4. The times are  $t=0$ s, 950s and 5000s.

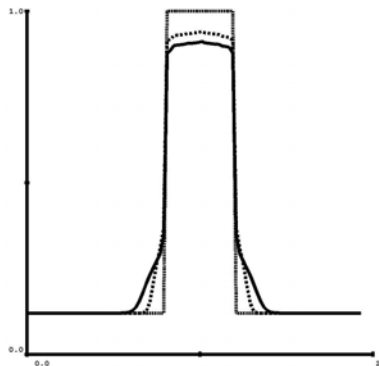


Figure 4. Saturation vs.  $x$  showing diffusion of a fully saturated region.

The diffusion rate gets slower with time because of the strong dependence of flow resistance with saturation. In this case, the flow resistance increases exponentially as the saturation is reduced.

For example, the flow resistance increases by a about a factor of two as the maximum saturation drops from 1.0 to 0.93. This trend can be seen in the rate at which the maximum saturation drops, which is much larger in the first 1000s (6% drop) than in the next 4000s (2% drop).

There is an important lesson in this example having to do with the distinction between unsaturated flow in a porous material versus a fully saturated flow with a free surface moving into porous material. Capillary pressures are always trying to pull liquid into the material against the flow resistance mounted by viscous stresses and the tortuosity of the material. If the flow resistance is sufficiently low, and enough liquid is available, then it is likely that a sharp interface (i.e., free surface) will exist between fully saturated and zero (or low) saturation conditions.

On the other hand, when the flow resistance is sufficiently large, the liquid may not be able to keep up with an advancing front and unsaturated conditions will result. Furthermore, if there is a fixed amount of total liquid, then with time it should spread out uniformly in the porous material. This is the case in the next example.

#### Drop Absorption in Porous Substrate

In this example a drop of water of diameter 1.0cm is placed on the surface of a 1.0cm thick piece of porous material having 10% porosity. The unsaturated flow properties of this material are:

$$\begin{aligned} \text{FPCMX} &= 0.1 \\ \text{PCMX} &= 5.0\text{E}+5 \\ \text{PEXP} &= 0.5 \\ \text{OADRG} &= 1.0\text{E}+4 \end{aligned}$$

The drop is quickly absorbed into the porous material and then is more slowly spread out over the material and is approaching a nearly uniform saturation, Figure 5.

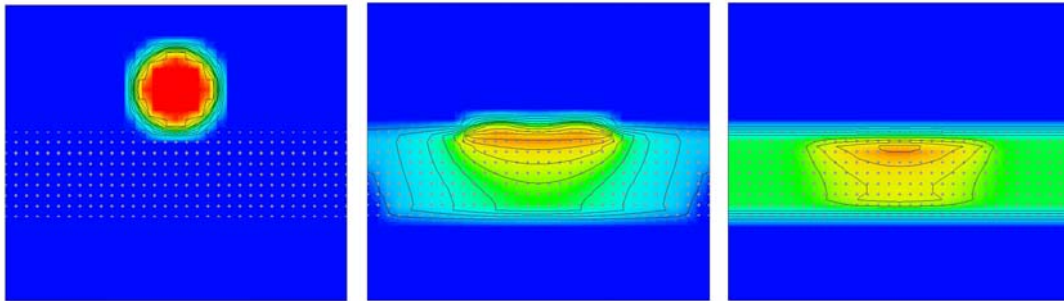


Figure 5. Absorption of liquid drop into a porous substrate,  $t=0.0\text{s}$ ,  $0.1\text{s}$  and  $1.0\text{s}$ .

#### **REMARKS**

The new model works well and is able to predict the results of a measured flow test. There are, however, several areas where additional development is desirable.

No attempt has been made to account for non-uniform porosities except for having separate porous regions (obstacles) each with its own porous media properties. More importantly, we have not tried to improve the scanning curves for capillary pressures between the draining and

filling curves. To do a better job with this there must be some decent experimental data available that can be used for guidance.

Additionally, some details regarding input parameters and material properties might be modified to make the unsaturated flow model more flexible.

## REFERENCES

1. Jacob Bear, *Dynamics of Fluids in Porous Media*, Dover Publications, Inc. NY, 1988
2. Nguyen, H.V. and Durso, D.F., *Absorption of Water by Fiber Webs: An Illustration of Diffusion Transport*, TAPPI Journal, pp.76-79, December 1983.
3. Gupta, R.P. and Staple, W.J., *Infiltration into Vertical Column of Soil Under a Small Positive Head*, Soil Science Proceedings, pp. 729-732, 1964.
4. Brooks, R.H. and Corey, A.T., *Properties of Porous Media Affecting Fluid Flow*, Journal of the Irrigation and Drainage Division, Proceedings of the ASCE, Vol. 92, pp.61-89, June 1966.
5. Gardener, W.R., *Solutions and Tests of the Diffusion Equation for the Movement of Water in Soil*, Soil Society Proceedings, pp.197-201, 1958.
6. Hayhoe, H.N., *Numerical Study of Quasi-Analytic and Finite Difference Solutions of the Soil-Water Transfer Equation*, Soil Science, Vol. 125, pp. 68-74, 1978.

## APPENDIX A – Nomenclature

<b>ADRG</b>	= Input parameter—Saturated drag (uniform throughout mesh)
<b>B</b>	= Exponent for unsaturated drag power-law (Input parameters <b>BDRG</b> or <b>OBDRG</b> )
<b>BDRG</b>	= Input parameter—Exponent for unsaturated drag power-law (uniform throughout mesh)
<b>d</b>	= Average particle diameter in solid
<b>DRG</b>	= Permeability variable used in <i>FLOW-3D</i> <sup>®</sup>
<b>F</b>	= Saturation, fraction of mesh cell volume filled with fluid
<b>F<sup>n</sup></b>	= Saturation in mesh cell at current time
<b>F<sup>n+1</sup></b>	= Saturation in mesh cell at new time level, <b>n+1</b>
<b>F<sub>AVE</sub></b>	= Average <b>F</b> value in neighboring cells
<b>F<sub>CMN</sub></b>	= Input variable –Irreducible saturation
<b>F<sub>PCMX</sub></b>	= Input parameter—Saturation at maximum capillary pressure <b>P<sub>CMX</sub></b>
<b>g</b>	= Gravitational vector
<b>IDFIT</b>	= Input parameter—Specifies form of drag-saturation relationship
<b>IDRG</b>	= Input parameter—Activates unsaturated flow in porous media model
<b>IPCFD</b>	= Input parameter—Controls hysteresis of capillary-saturation relationship
<b>K</b>	= Drag (units =s <sup>-1</sup> )
<b>K0</b>	= Saturated drag (units =s <sup>-1</sup> )
<b>N, VF</b>	= Porosity, Open Volume/Total Volume
<b>OADR</b>	= Input parameter—Saturated drag for a particular obstacle
<b>OBDRG</b>	= Input parameter—Exponent for unsaturated drag power-law for a particular obstacle
<b>p</b>	= Pressure in mesh cell at new time level, <b>n+1</b>
<b>p<sup>n</sup></b>	= Pressure in mesh cell at current time

$P_b$	= “Bubbling” pressure
$P_c$	= Capillary pressure
$P_{CMX}$	= Maximum capillary pressure
$P$	= Capillary pressure at current saturation
$P^{n+1}$	= Anticipated capillary pressure at new time level, <b>n+1</b>
$P_c$	= Capillary pressure from filling curve
$P_{exp}$	= Exponent for capillary pressure-saturation relationship
<b>PVOID</b>	= Input parameter—Void Pressure
$S_e$	= Effective saturation, $(F-F_{CMN})/(1-F_{CMN})$
$v$	= Velocity vector
$u$	= Wetting front velocity
$u^n$	= Fluid velocity at current time
$u^{n+1}$	= Fluid velocity at new time level, <b>n+1</b>
<b>VF,n</b>	= Porosity
$\delta t$	= Time step, <b>Time<sup>n+1</sup>-Time<sup>n</sup></b>
$\delta x$	= Mesh cell length
$\rho$	= Fluid density
$\nu$	= Fluid kinematic viscosity

## APPENDIX B – Nomenclature—Input Variables

### Namelist XPUT

Variable	Default	Description
<b>ADRG</b>	0.0	Drag in saturated flow (independent of obstacle number)
<b>BDRG</b>	0.0	Exponent for unsaturated drag (independent of obstacle number)
<b>IDRG</b>	0	Drag, function flag =5, unsaturated flow in porous media

### Namelist PCAP

Variable	Default	Description
<b>FCMN</b>	0.0	Irreducible saturation (minimum <b>F</b> value—must be less than <b>FPCMX</b> )
<b>FCMX</b>	1.0	Fully saturated F value
<b>FPCMX</b>	...	<b>F</b> value corresponding to <b>PCMX</b>
<b>IDFIT</b>	0	Drag function flag—relationship between drag and saturation
<b>IPCFD</b>	0	Capillary pressure operation mode =0, use filling and draining curves (hysteresis effects) =1, drive pressures to filling curve =2, drive pressures to draining curve
<b>PCMX</b>	...	Maximum capillary pressure at <b>F=FPCMX</b>
<b>PEXP</b>	...	Exponent for capillary pressure-saturation relationship

### Namelist OBS

<b>Variable</b>	<b>Default</b>	<b>Description</b>
<b>OADR<math>G(n)</math></b>	0.0	Drag in saturated flow (for obstacle number <b>n</b> )
<b>OBDR<math>G(n)</math></b>	0.0	Exponent for unsaturated drag (for obstacle number <b>n</b> )